Journal of Applied Fluid Mechanics, Vol. 8, No. 4, pp. 855-862, 2015.
Available online at www.jafmonline.net, ISSN 1735-3572, EISSN 1735-3645.
DOI: 10.18869/acadpub.jafm.73.238.23277

Investigating Flat Plate Drag Reduction Using Taguchi Robust Design

G. Ghassabi and M. Kahrom†

Department of Mechanical Engineering, Ferdowsi University of Mashhad, Mashhad, Iran

†*Corresponding Author Email: mkahrom@ferdowsi.um.ac.ir*

(Received June 2, 2014; accepted September 18, 2014)

ABSTRACT

Research has shown when a rectangular cylinder is located near a flat plate, the flat plate skin friction coefficient changes as a function of the rectangular aspect ratio, gap height between the rectangular and flat plate, distance of rectangular from the flat plate leading edge, and speed of free stream. However, there is no comprehensive experimental study on the comparison of the results of the flat plate skin friction coefficient for all the interactions between effective variables in the presence and absence of the obstacle. On the other hand, testing all possible combinations of effective variables will not be reasonable. In this paper, maximum and minimum ratios of the flat plate skin friction coefficients with and without the rectangular cylinder were determined using robust Taguchi design. Design of experiments method was applied for decreasing the number of experiments without losing the required information in the first step. Then, experimentation was done in a wind tunnel, the maximum speed of which was 13 m/s. Finally, the flat plate skin friction coefficient was optimized using Taguchi method and Minitab software. Results showed that presence of the rectangular cylinder near the flat plate decreased the average skin friction coefficient of the flat plate for all the possible combinations of the effective variables. Additionally, maximum value of the flat plate skin friction reduction was about 40%.

Keywords: Skin friction coefficient; Drag reduction; Design of experiments; Taguchi method; Rectangular cylinder.

NOMENCLATURE

A	flat plate area	Re_t	Reynolds number based on cylinder thickness
C	length of the rectangular cylinder	t	thickness of the rectangular cylinder
d	gap height between the rectangular cylinder and flat plate	U_∞	speed of free stream
F	skin friction force	ρ	density of air
H	length of Flat plate	μ	viscosity of air
L	distance of the rectangular cylinder from the flat plate leading edge	η	signal-to-noise (S/N) ratio
LV	levels	$\overline{\eta}_i$	mean of S/N ratio at optimum levels
$N_{Taguchi}$	minimum number of experiment to be conducted for Taguchi method	η_m	mean of S/N ratio
Re_H	Reynolds number based on length of flat plate		

1. INTRODUCTION

The amount of fuel consumption of vehicles has been an important issue in recent years. Frictional drag reduction of vehicles is one of the most important factors for decreasing fuel consumption, Kourta and Gilliéron (2009). Numerous methods have investigated decreasing the frictional drag; one of the simple ones is inserting an obstacle inside a boundary layer, Bruneau et al. (2012). By doing so, a stagnation point is formed over the frontal area of the insert geometry, providing a driving force to push the flow stream from the gap between the obstacle and wall. The jet passing through the gap is a cause of vortex generation at downstream to the obstacle which in turn makes considerable contribution to the skin friction reduction, as reported by, Inaoka et al. (1998), de Souza et al. (1999) and Ghassabi and Kahrom (2013). Also, Marumo et al. (1985) compared the value of skin friction coefficient of the flat plate with and without circular cylinder insert near the plate. Their results showed that skin friction coefficient decreased in the presence of the obstacle. This result was also

given by other researchers for circular cylinder, Suzuki et al. (1988) and Suzuki and Suzuki (1991). Inaoka et al. (1999) placed a square insert in the turbulent boundary layer and measured the skin friction coefficient. Their results represented that skin friction coefficient was reduced by inserting this insert. They also found the same result for the laminar flow, Inaoka et al. (1998).

Some researchers have studied the effect of insert geometric parameters on the skin friction coefficient. Kahrom et al. (2010) optimized the dimension of a quad insert and the gap height that provided maximum heat transfer and minimum skin friction coefficients. Suzuki and Suzuki (1991) studied effect of the circular cylinder size and gap height on the skin friction coefficient of the flat plate.

This study indicated that gap height was more effective than cylinder size in skin friction coefficient. Also, Sarkar and Sarkar (2010) observed that gap height had a strong influence on shear layer when a circular cylinder was located near the wall. Therefore, researches have shown that skin friction coefficient changes as a function of the obstacle aspect ratio and gap height when an obstacle is located near the wall. However, there is no comprehensive experimental study on the comparison of the results of the flat plate skin friction coefficient for all the interactions between effective variables in the presence and absence of the obstacle. On the other hand, testing all the possible combinations of effective variables will not be reasonable.

The present study aimed to determine optimal conditions that provided minimum and maximum values for the average flat plate skin friction coefficients between all the possible combinations of effective variables in the presence of the rectangular cylinder insert. For this purpose, first, the average skin friction coefficients were calculated experimentally as a function of effective variables.

Also, design of experiments (DOE) method was used for decreasing the number of experiments without losing the required information. Then, Taguchi method was applied for determining maximum and minimum values of the average skin friction coefficients in the presence of the rectangular cylinder insert using Minitab software. Results showed that the rectangular cylinder insert decreased the average skin friction coefficient of flat plate for all the possible combination of effective variables.

2. PROBLEM DEFINITION

When a rectangular cylinder is located near a flat plate as shown in Fig. 1, depending on its dimensions (C, t), its distance from the flat plate leading edge (L), gap height between the rectangular cylinder and flat plate (d), and speed of free stream (U_∞),deformation of the boundary layer is specified.

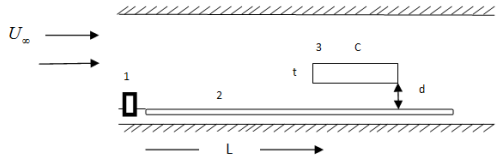

Fig. 1. Description of the experimental set up (1-Load cell, 2-Floating surface, 3-Rectangular cylinder).

Thus, the obstacle creates a specific distribution of the skin friction coefficients over the flat plate for each configuration at a special speed, Kahrom et al. (2010). Therefore, the average skin friction coefficient introduced in Eq. (1) is a function of the mentioned parameters. (Eq. (2))

$$\overline{C_f} = \frac{1}{H}\int_0^H C_f\,dx = \frac{F}{\frac{1}{2}\rho U_\infty{}^2 A} \tag{1}$$

$$\overline{C_f} = \mathrm{f}(L, C, t, d, U_\infty, \rho, \mu) \tag{2}$$

By dimensional analysis, the non-dimensional groups of Eq. (2) are:

$$\overline{C_f} = \mathrm{f}(L/t,\ C/t,\ d/t,\ \mathrm{Re}_t = \rho U_\infty t/\mu) \tag{3}$$

These variables can change in an extensive range. Furthermore, if all the interactions between the independent variables are investigated, doing a large number of experiments is required. Thus, for decreasing the number of experiments so that all the required information would not be lost, design of experiments method was used in the present study.

3. EXPERIMENTAL SET UP

Experiments were performed in the subsonic open-circuit wind tunnel with a test section with the following dimensions: 0.3 m (height)× 0.3m (width) × 2m (length). In the test section, maximum speed was 13m/s and the turbulence intensity of uniform free stream was less than 1.0% so that it can be assumed that flow was laminar in the inlet. However, based on length of flat plate and value of critical Reynolds number (5× 10^5), flow became fully turbulent in the downstream region. the Dimension of the rectangular cylinder was C (length)× 0.3m(width)× t (thickness) mounted normal to free stream direction and was placed d from the bottom of the test section and L from the test section leading edge, as shown in Fig. 1. Thickness of the rectangular was fixed at 8 mm and change of aspect ratio was done by changing the rectangular length. Floating-frame balance method was used for calculating the average skin friction coefficient of the flat plate, Naughton and Sheplak (2002). Friction forces were measured by a load cell with 0.01 gr accuracy, which was connected to the leading edge of the floating surface, as shown in Fig. 1 and Fig. 2.

4. DESIGN OF EXPERIMENTS

Design of experiments is a procedure for generating the required information with the minimum amount of experimentation based on statistical methods, Rajabi and Kadkhodayan (2013). Several DOE

methods have been developed in the recent years. One of the most popular DOE methods is Taguchi method. This method creates an optimal combination of interaction between independent variables which maximizes sensitivity by a minimum number of experiments. The experimental design proposed by Taguchi involves using orthogonal arrays to organize the independent variables affecting the process and levels at which they should be varied. Instead of having to test all the possible combinations like factorial design, the Taguchi method tests pairs of combinations, which allows for collecting the necessary data to determine which factors have the highest effect on the dependent variable with the minimum amount of experimentation; thus, saving time and resources, Singh and Batra (2013). The first step in the Taguchi method is selection of the levels of the independent variables. Levels of (d/t) is determined Based on results of Price et al. (2002). Their results showed the existence of four distinct flow regimes as the cylinder-wall gap size is varied: a) The very small gap flow regime (d/t≤0.125) in which vortex shedding is suppressed; b) The small gap flow regime (0.125<d/t<0.5) in which the flow pattern is similar to those of d/t ≤0.125 with the exception of a pronounced pairing between the lower shear layer separated from the bottom side of the cylinder and the wall boundary layer; c) The intermediate gap flow regime (0.5≤d/t<0.75) in which vortex shedding becomes intermittent; d) The large gap flow regime (d/t>0.75) in which there is no separation of the wall boundary layer. Therefore, four levels were considered for d/t, as shown in Table 1.

Fig. 2. Configuration of load cell and floating surface.

Table 1 Levels of independent variables

Variable	Level-1	Level-2	Level-3	Level-4
Re_t	5384.8	5920.02	6455.23	7525.67
C/t	2	4	8	18
d/t	0.125	0.25	0. 5	1
L/t	37.5	175	-	-

To study aspect ratio effect of the rectangular cylinder on $\overline{C_f}$, C/t was defined as an independent variable. For selection of C/t levels, results of Parker and M.C.Welsht (1983) were used. They suggest that there exist four possible vortex shedding regimes for rectangular cylinders, depending on the chord-to-thickness ratio (C/t). Stokes and Welsh (1986) summarized these as follows:(a) C/t<3.2: the leading-edge shear layers interact directly in the wake to form a Karman-like vortex street; (b) 3.2<C/t<7.6: the leading-edge shear layers reattach to the plate periodically; following reattachment the separation bubble grows beyond the trailing edge and a regular vortex street is usually observed; (c) 7.6<C/t<16: the leading-edge shear layers always reattach upstream of the trailing edge; the separation bubble tends to grow and divide in a random manner and discrete vortices are generated; Shadaram et al. (2007). These vortices arrive at the trailing edge randomly and interfere with the trailing-edge separation, and no regular shedding is observed; (d) C/t>16: the vortices shed from the separation bubble are diffused upstream of the trailing edge, where the developing boundary layers separate and interact in the wake to form a Karman-like vortex street. Thus, four levels were selected for C/t presented in Table 1.In order to consider effects of both laminar and turbulent regions of the flat plat boundary layer on $\overline{C_f}$, two levels were defined for L/t demonstrated in Table 1. Selection of Re_t number levels is based on limitations of the experimental set up. Re_t number levels are also showed in Table 1.

In the second step, configurations of the experiments were achieved using fractional factorial test designs called orthogonal arrays. The orthogonal arrays available are L_4, L_8, L_9, L_{12}, L_{16}, L_{18}, L_{32}, etc. Before selecting an orthogonal array, the minimum number of experiments to be conducted can be fixed by using the following relation, Sivasakthivel et al. (2014):

$$N_{\text{Taguchi}} = 1 + \sum_{i=1}^{P} (LV - 1) \tag{4}$$

In Eq. (4), P represents the number of independent variables. In the present study, one independent variable having two levels and the other having three levels, as shown in Table 1. Therefore, minimum number of experiments required based on Eq. (4) is 11. Hence, L_{12}, L_{16}, L_{18}, L_{32} can be chosen. To improve the accuracy of results, L_{32} orthogonal array was employed and structure of the array is demonstrated in Table 2.

5. DETERMINING OPTIMAL CONDITIONS USING TAGUCHI ROBUST DESIGN

One of the most applicable methods for the optimization of a function in experimental studies is the Taguchi method,Gardiner and Gettinby (1998). The Taguchi method uses the S/N ratio to measure the quality characteristic deviating from the desired value,Singh and Batra (2013). The terms ‘signal’ and ‘noise’ represent the desirable and undesirable values for the output characteristics, respectively. There are three categories of quality characteristics in the analysis of the S/N ratio: the lower the better (L.B.), nominal is best (N.B.), and the higher the better (H.B.),Gardiner and Gettinby (1998). Based on what was mentioned in the introduction, the

Table 2 Designed experiments and S/N ratios

Experiment	C/t	d/t	Re_t	L/t	S/N ratio(dB)-H.B.	S/N ratio(dB)-L.B.
1	2	0.125	5384.80	175.00	-1.57013	1.57013
2	2	0.250	5920.02	175.00	-2.13671	2.13671
3	2	0.500	6455.23	175.00	-1.00504	1.005038
4	2	1.000	7525.67	175.00	-0.05102	0.051019
5	4	0.125	5384.80	175.00	-2.07711	2.077108
6	4	0.250	5920.02	175.00	-2.33143	2.331432
7	4	0.500	6455.23	175.00	-1.17617	1.176172
8	4	1.000	7525.67	175.00	-0.65417	0.654172
9	8	0.125	5920.02	175.00	-1.57309	1.573091
10	8	0.250	5384.80	175.00	-2.61795	2.617947
11	8	0.500	7525.67	175.00	-1.17292	1.17292
12	8	1.000	6455.23	175.00	-0.60383	0.603834
13	18	0.125	5920.02	175.00	-1.76878	1.768782
14	18	0.250	5384.80	175.00	-3.67442	3.674422
15	18	0.500	7525.67	175.00	-1.54319	1.543187
16	18	1.000	6455.23	175.00	-0.9401	0.940104
17	2	0.125	7525.67	37.50	-1.63948	1.639484
18	2	0.250	6455.23	37.50	-1.33719	1.337192
19	2	0.500	5920.02	37.50	-0.22826	0.228256
20	2	1.000	5384.80	37.50	-0.32789	0.327889
21	4	0.125	7525.67	37.50	-1.73441	1.734413
22	4	0.250	6455.23	37.50	-1.37112	1.371117
23	4	0.500	5920.02	37.50	-0.23757	0.237572
24	4	1.000	5384.80	37.50	-0.66617	0.666171
25	8	0.125	6455.23	37.50	-2.84709	2.847093
26	8	0.250	7525.67	37.50	-1.40543	1.405426
27	8	0.500	5384.80	37.50	-1.28664	1.28664
28	8	1.000	5920.02	37.50	-0.05311	0.053112
29	18	0.125	6455.23	37.50	-3.06466	3.06466
30	18	0.250	7525.67	37.50	-1.4243	1.424298
31	18	0.500	5384.80	37.50	-1.48666	1.486663
32	18	1.000	5920.02	37.50	-0.78784	0.787837

lower the better and the higher the better categories were used in this paper. For these categories, the formulas used for calculating S/N ratio of *N* repeated experiments are given in following equations:

$$\eta_{L.B} = -10Log(\frac{1}{N}\sum_{m=1}^{N} {y_m}^2) \quad (5)$$

$$\eta_{H.B} = -10Log(\frac{1}{N}\sum_{m=1}^{N} \frac{1}{{y_m}^2}) \quad (6)$$

Where y_m is the value of the experiment output and Unit of S/N ratio is decibel (dB).

As better performance is indicated by greater values of S/N ratio, optimum levels occur at the levels with maximum S/N ratio for each factor. S/N ratio for optimal levels is calculated by Eq. (7):

$$\eta = \eta_m + \sum_{i=1}^{p}(\bar{\eta}_i - \eta_m) \quad (7)$$

In Eq. (7), P represents the number of independent variables. Then, predicted value of skin friction coefficient for optimum levels is given using the following equations:

$$X_{L.B} = \sqrt{10^{-\frac{\eta}{10}}} \quad (8)$$

$$X_{H.B} = \sqrt{10^{\frac{\eta}{10}}} \quad (9)$$

6. RESULTS AND DISCUSSION

To establish the accuracy of the present study, the comparison of $\overline{C_f}$ in the absence of the cylinder between the empirical equation, Bergman et al. (2011) mentioned in Eq. (10) and experimental data is presented in Fig. 3 for four Reynolds numbers based on length of flat plate. It is observed that experimental results are in good agreement with the data from the Eq. (10).

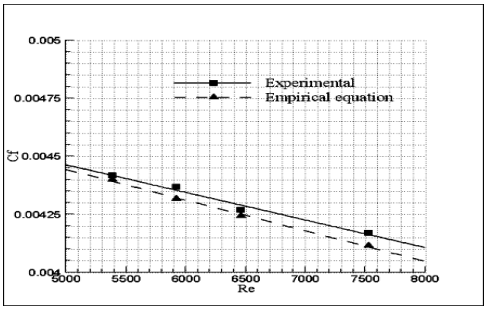

Fig. 3. Comparison of $\overline{C_f}$ between the empirical equation and experimental data.

$$\overline{C_f} = 0.074\,\mathrm{Re}_H^{\frac{-1}{5}} - \frac{1742}{\mathrm{Re}_H} \qquad (10)$$

Ratios of the flat plate skin friction coefficients with and without the rectangular cylinder insert for all the designed experiments are presented in Table 3. It can be seen that ratios of the skin friction coefficients are less than one for all the experiments. Therefore, the skin friction coefficient decreases for all the designed experiments by inserting the rectangular cylinder near the flat plate.

Table 3 Ratio of skin friction coefficients

Experiment	$\overline{C_f}$ ratio
1	0.834629
2	0.781924
3	0.890734
4	0.994143
5	0.787308
6	0.76459
7	0.873356
8	0.927452
9	0.834345
10	0.73978
11	0.873683
12	0.932842
13	0.815757
14	0.655057
15	0.837222
16	0.897418
17	0.827991
18	0.857315
19	0.974063
20	0.962954
21	0.818991
22	0.853973
23	0.973019
24	0.926172
25	0.720519
26	0.850607
27	0.862319
28	0.993904
29	0.702695
30	0.84876
31	0.842688
32	0.913289

To confirm this result for all the possible combinations of effective variables, it would be enough for the maximum value of the flat plate skin friction coefficients ratio with and without rectangular cylinder insert to become less than one between all the possible configurations of experiments. For this purpose, the higher the better category of the Taguchi method was used by Minitab software for determining the maximum ratio of the flat plate skin friction coefficients. Minitab is statistical and graphical analysis software for Windows. Minitab can perform a wide variety of tasks, from the construction of graphical and numerical summaries for a set of data to the more complicated statistical procedures, Chowdhury et al. (2014).

Values of S/N ratio for the designed experiments are presented in Table 2. By averaging the S/N ratios for each factor at a special level, a graph is made, as shown in Fig. 4 and Fig. 5. For instance, average S/N for the first level of (L/t) was calculated by averaging S/N ratio for rows 1 to 16 in Table 2, where the level of factor *(*L/t*)* is at level 1. Based on Fig. 4, optimum levels were obtained at the second level of (L/t), first level of (C/t), forth level of (d/t) and second level of (Re_t) for the higher the better criterion.

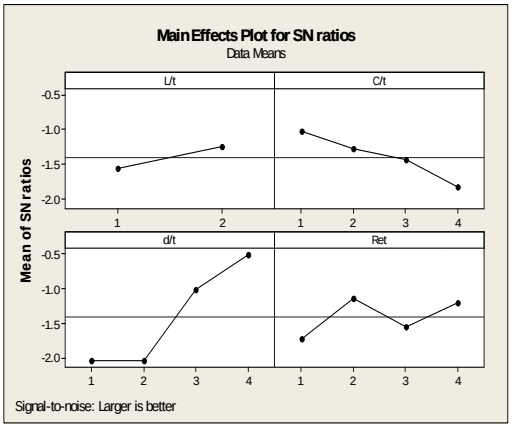

Fig. 4. Average of the S/N ratios for each factor for the higher the better criterion.

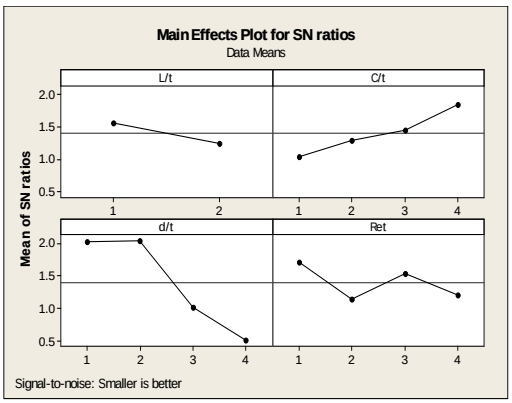

Fig. 5. Average of the S/N ratios for each factor based on the lower the better criterion.

In Fig. 5, average of the S/N ratios is presented for each factor based on the lower the better criterion. It can be seen that minimum value of the flat plate

Table 4 Comparison of experimental and predicted values of $\overline{C_f}$ ratios for optimum levels

Category	Predicted	Experimental
H.B.	0.998473	0.997643
L.B.	0.61321	0.60564

Table 5 ANOVA of S/N ratios

Source	D.F.	SeqSS	AdjSS	AdjMS	F-value	P-value
L/t	1	0.7807	0.7807	0.7807	3.55	0.074
C/t	3	2.7063	2.7063	0.9021	4.10	0.019
d/t	3	13.9711	13.9711	4.6570	21.17	0.000
Ret	3	1.8021	1.8021	0.6007	2.73	0.070
Error	21	4.6205	4.6205	0.2200		
Total	31	23.8807				

skin friction coefficient was obtained at the first level of (L/t), forth level of (C/t), second level of (d/t), and first level of (Re_t). It could be inferred that the maximum value of drag reduction occurred in the turbulent region of the boundary layer, which could be attributed to that the velocity gradient near the plate for the turbulent region of the boundary layer is much larger than that of the laminar region, Bergman et al. (2011). Also, optimum level of (d/t) is 0.25, as reported in Kahrom et al. (2010). Moreover, it is observed that S/N ratio increases as (C/t) increases. It could be inferred that drag reduction increases as (C/t) increases, which could be attributed to that reveres flow behind of the rectangular cylinder near the flat plate become larger and stronger when (C/t) increases, Kahrom et al. (2010).

Comparison of the experimental and predicted ratios of flat plate skin friction coefficients with and without the rectangular cylinder insert are presented in Table 4 for optimum levels. It can be observed that the predicted values were in good agreement with the experimental data. Furthermore, as demonstrated in the table, the predicted and experimental values of maximum ratio of $\overline{C_f}$ were less than one, implying that the rectangular cylinder insert decreased the average skin friction coefficient of flat plate for all the combinations of effective variables. Also, it could be observed that the maximum value of the flat plate skin friction reduction was about 40%.

In Table 5, Analysis of Variance (ANOVA) is shown for S/N ratios. In this table, AdjMS_i determines adjusted mean sum of squares for factor *i* and is defined as, Akbarzadeh et al. (2013):

$$AdjMS_i = \frac{AdjSS_i}{D.F._i} \tag{11}$$

where AdjSS_i and $D.F._i$ are adjusted sum of squares and degree of freedom for factor *i*, respectively, $D.F._i$ is equal to the number of levels minus one for each factor, total D.F. is number of experiments minus one, and degree of freedom, D.F., for error is the difference between total D.F. and sum of $D.F._i$ for all input factors. F- and P-values for independent variables can be observed in this table as well. F-value for factor i is defined as, Akbarzadeh et al. (2013):

$$F-value = \frac{AdjMS_i}{AdjMS_E} \tag{12}$$

where AdjMS_E is adjusted mean sum of squares for error. Degree of significance of F-value can be determined by looking up F-tables. Larger F-value shows that the variation of the parameter has a larger impact on the output performance characteristics, Akbarzadeh et al. (2013). Therefore, when F-value of a parameter is larger than $F_{\alpha,v1,v2}$ - value provided by the confidence table, then it can be concluded that the parameter is significant. Variables *α, v*1 and *v*2 are risk, degrees of freedom (D.F.) associated with input factor, and error, respectively. Additionally, if P-value is less than or equal to the selected α, then effect of the variable is significant. A detailed explanation of these statistical terms is described in study of Akbarzadeh et al. (2013). Based on the confidence level 95%, i.e. α is set at 0.05 and the confidence table, (d/t) is the most significant variable for the trend of $\overline{C_f}$, this is due to that the gap height possesses the highest F-value and minimum P-value. However, (L/t) has the least effect on it, since it has the maximum P-value.

7. CONCLUSION

In this paper, the flow over a rectangular cylinder near a flat plate was experimentally studied for calculating the average skin friction coefficient of flat plate as a function of all effective variables including gap height, rectangular aspect ratio, distance of rectangular from the flat plate leading edge, and speed of free stream. Also, design of experiments method was applied for decreasing the number of experiments without losing the required information. Then, maximum and minimum ratio of the flat plate skin friction coefficients with and without the rectangular cylinder insert was determined using the robust Taguchi design. The following conclusions were obtained from the analysis of the results:

1. Maximum flat plate skin friction reduction occurred in the turbulent region of the boundary layer and d/t of 0.25.
2. Maximum value of the flat plate skin friction reduction was about 40%.
3. Gap height was the most effective variable in the trend of the average skin friction

coefficient of flat plate. However, distance of rectangular from the flat plate leading edge had the least effect.

4. The rectangular cylinder insert decreased the average skin friction coefficient of the flat plate for all the possible combinations of effective variables.

REFERENCES

Akbarzadeh, A., S. Kouravand and B. M. Imani (2013). Robust Design of a Bimetallic Micro Thermal Sensor Using Taguchi Method. *Journal of Optimization Theory and Applications* 157(1),188-198.

Bergman, T. L., A. S. Lavine, F. P. Incropera and D. P. Dewitt (2011). *Fundamentals of Heat and Mass Transfer*. United States of America. John Wiley & Sons.

Bruneau, C.H., E. Creusé, D. Depeyras, P. Gilliéron and I. Mortazavi (2012). Active and Passive Flow Control around Simplified Ground Vehicles. *journal of Applied Fluid Mechanics* 5(1),89-93.

Chowdhury, A., R. Chakraborty, D. Mitra and D. Biswasa (2014). Optimization of the production parameters of octyl ester biolubricant using Taguchi's design method and physico-chemical characterizationof the product. *Industrial Crops and Products,* 52(Jun.) 783– 789.

DeSouza, F., J. Delville, J. Lewalle and J. P. Bonnet (1999). Large Scale Coherent Structures in a Turbulent Boundary Layer Interacting with a Cylinder Wake. *Experimental Thermal and Fluid Science* 19(4),204-213.

Gardiner, W. P. and G. Gettinby (1998). *Experimental Design Techniques in Statistical Practic*. Glasgow. Woodhead.

Ghassabi, G. and M. Kahrom (2013). Optimization of Heat Transfer Enhancement of a Domestic Gas Burner Based on Pareto Genetic Algorithm: Experimental and Numerical Approach. *International Journal of Engineering* 26(1),469- 481.

Inaoka, K., M. Mesaru and K. Suzuki (1998). Flow and Heat Transfer Characteristics of a Turbulent Boundary Layer with an Insertion of a Square Rod(Control of Vortex Shedding by a Splitter Plate). *Transactions of the Japan Society of Mechanical Engineers* 97(4),212-218.

Inaoka, K., J. Yamamoto and K. Suzuki (1998). Heat Transfer Characteristics of a Flat Plate Laminar Boundary Layer Disturbed by a Square Rod. *International conference on advanced computational methods in heat transfer* Kraków, Poland 297-306.

Inaoka, K., J. Yamamoto and K. Suzuki (1999). Dissimilarity Between Heat Transfer and Momentum Transfer in a Disturbed Turbulent Boundary Layer with Insertion of a Rod-Modeling and Numerical Simulation. *International Journal of Heat and Fluid Flow* 20(3),290-301.

Kahrom, M., P. Haghparast and S.M. Javadi (2010). Optimization of Heat Transfer Enhancement of a Flat Plate Based on Pareto Genetic Algorithm *international Journal of Engineering* 23(2),177-189.

Kahrom, M., B. Zafarmand, S. M. Javadi and A. Exier (2010). Heat Transfer Enhansement from a Flat Plate by Vortex Shedding Behind aTriangular Obstacle. *Amir Kabir Mechanical Engineering* 41(2),37-46.

Kourta, A. and P. Gilliéron (2009). Impact of the Automotive Aerodynamic Control on the Economic Issues. *Journal of Applied Fluid Mechanics* 2(2),69-75.

Marumo, E., K. Suzukit and T. Satot (1985). Turbulent Heat Transfer in a Flat Plate Boundary Layer Disturbed by a Cylinder. *International Journal of Heat and Fluid Flow* 6(4),241-248.

Naughton, J. W. and M. Sheplak (2002). Modern Developments in Shear Stress Measurement. *Progress in Aerospace Sciences* 38(6-7),515–570.

Parker, R. and M.C.Welsht (1983). Effects of Sound on Flow Separation from Blunt Flat Plates. *International of Journal of Heat and Fluid Flow* 4(2),113-127.

Price, S. J., D. Sumner, J. G. Smith, K. Leong and M. P. Paigdoussis (2002). Flow Visualization around a Circular Cylinder Near to a Plane Wall *Journal of Fluids and Structures* 16(2),175-191.

Rajabi, A. and M. Kadkhodayan (2013). An Investigation Into The Deep Drawing of Fiber-Metal Laminates Based On Glass Fiber Reinforced Polypropylene. *International Journal of Engineering* 27(3),349-358.

Sarkar, S. and S. Sarkar (2010). Vortex Dynamics of a Cylinder Wake in Proximity to a Wall. *Journal of Fluids and Structures* 26(1),19–40.

Shadaram, A., M. Azimi-Fard and N. Rostamy (2007). Experimental Study of the Characteristics of the Flow in the Near Wake of a Rectangular Cylinder. *Aerospace Mechanics Journal* 3(3),13-23.

Singh, R. P. and U. Batra (2013). Effect of Cold Spraying Parameters and Their Interaction an Hydroxyapatite Deposition. *Journal of Applied*

Fluid Mechanics, 6(4),555-561.

Sivasakthivel, T., K. Murugesan and H.R. Thomas (2014). Optimization of operating parameters of ground source heat pump system for space heating and cooling by Taguchi method and utility concept. *Applied Energy* 116(Mar.), 76–85.

Stokes, A. N. and M. C. Welsh (1986). Flow-Resonant Sound Interaction in a Duct Containing a Plate, II: Square Leading Edge. *Journal of Sound and Vibration* 104 (1),55-73.

Suzuki, H. and K. Suzuki (1991). Heat Transfer and Skin Friction of a Flat Plate Turbulent Boundary Layer Disturbed by a Cylinder. *Heat Transfer - Japanese Research* 20(2),97-112.

Suzuki, H., K. Suzuki and T. Sato (1988). Dissimilarity Between Heat and Momentum Transfer in a Turbulent Boundary Disturbed by a Cylinder Layer. *International Journal of Heat and Mass Transfer* 31(2),259-265.